Toward a Subhourly Net Zero Energy District Design Through Integrated Building and Distribution System Modeling

Kate Doubleday,[1,2] Andrew Parker,[3] Faeza Hafiz,[1,4] Benjamin Irwin,[5] Samuel Hancock,[5] Shanti Pless,[3] and Bri-Mathias Hodge[1,2,a)]

[1)] *Power Systems Engineering Center, National Renewable Energy Laboratory*
[2)] *Electrical, Computer, and Energy Engineering Department, and Renewable & Sustainable Energy Institute, University of Colorado Boulder*
[3)] *Building and Thermal Sciences Center, National Renewable Energy Laboratory*
[4)] *Electrical and Computer Engineering Department, North Carolina State University*
[5)] *Xcel Energy*

(Dated: 10 May 2019)

A modeling framework integrating both building energy modeling and power systems modeling is introduced for the design of net zero energy (NZE) districts for the simultaneous selection of both demand-side efficiency measures and supply-side generation technologies. A novel district control scheme is proposed for pursuing NZE on a subhourly basis while mitigating potential grid impacts such as power backfeeding and voltage violations. As a case study, Peña Station NEXT, a new 100-building, mixed-use district on a 1,200-node distribution feeder in Denver, Colorado, is modeled in the integrated framework. An exhaustive scenario analysis is conducted for sizing the district's distributed energy resources, considering multiple objectives such as capital cost, net energy import, and equipment violations. When trying to achieve annual NZE, the district incurs frequent operating violations, and achieving NZE on a 15-minute basis is also limited by seasonal fluctuations in photovoltaic output, illustrating the need for diverse generation or seasonal storage. As a practical compromise, both annual and 15-minute district import can be reduced ∼78% without significant violations.

I. INTRODUCTION

Rising global interest in greenhouse gas reductions and energy conservation is spurring the development of sustainable communities and smart cities.[1] One expression of this trend is the net zero energy (NZE) district or town, which on average produces enough energy on-site to offset its consumption, typically balanced over an annual time horizon.[2,3] In addition to grassroots support for community sustainability, the idea of the NZE district also has governmental support, for example through the U.S. Department of Energy's Zero Energy District Accelerator.[4]

To achieve NZE, these communities generally employ high-efficiency building measures and distributed energy resources (DERs), such as solar photovoltaics (PV); however, the sustainable and NZE district planning process typically does not include consideration of the electric distribution system and assumes that the grid can accommodate any magnitude of power import or export at any time.[5] Even when a finer hourly or subhourly time resolution is considered, the distribution system is often excluded or much simplified.[6,7] Neglecting grid impacts from high DER penetrations during the design phase can result in a variety of complications, including power backfeeding, voltage violations, and inappropriate protective equipment responses. As a result, the district developer might be faced with costly infrastructure reinforcements or unanticipated DER curtailment that interferes with the district's ability to achieve NZE in practice.[8]

Centralized planning of a district's buildings and distribution system, including its DERs and their operational impacts, could mitigate these challenges and improve NZE performance. One approach is for electric utilities and district developers to work together during the design process to establish interconnection requirements that meet the needs of both parties. An alternative approach is for utilities to own and operate DERs directly through rate-based investments, which is not necessary for coordinated DER control but can certainly facilitate it. This is not yet common in practice, as most DERs are currently owned and operated by end-users or third parties. However, a recent survey of ∼700 American and Canadian utility employees indicates 50% support the option of utility DER ownership through rate-based investments, an option that may simplify management of variable and uncertain generation to maintain reliable service.[9] For example, this model may be of interest to Xcel Energy, an electric utility that recently committed to providing 100% carbon-free electricity by 2050,[10] and which serves the case study district described below.

In the context of NZE districts, such an ownership model may be agreeable to the multiple stakeholders. The district's residents can meet their sustainability goals by agreeing to a specialized rate-case funding the district's very high penetration of renewable DERs, while the utility can take direct management to ensure reliable service and avoid detrimental power quality impacts on its other customers. While the design of such a rate-case is beyond the current scope, the aim of the current work is to provide the technical analysis to find promising district designs, with a particular focus on the DER build-out, which can in turn inform the final market structure.

[a)] bri.mathias.hodge@nrel.gov

To facilitate the centralized NZE district design, the building and distribution system models can be integrated into one framework to enable developers and system operators to compare investment in demand-side technologies (e.g., energy efficiency, demand response) with supply-side technologies (e.g., renewable DERs, electrical energy storage systems (ESS), smart inverters) to determine possible system architectures; however, advances in data-driven modeling and new control schemes are required from the research community to enable highly detailed integrated district planning, especially when improving the design process to consider operations.

Most district design processes have excluded detailed distribution system models, but recent modeling frameworks have started to address this gap. Morvaj et al.[11,12] present a planning and operations optimization tool incorporating building simulations in EnergyPlus with distribution grid models. Another such framework is MESCOS, which interfaces commercial software to model building loads; system controls; and gas, heat, and electricity networks.[13] In Kusakiyo et al. and Fujimoto et al.,[14,15] PV generation and building loads are modeled endogenously based on occupant activity data. The IDEAS library also models building activities and loads, thermal systems, DERs, the distribution grid, and various controls endogenously.[8,16,17] These previous works have applied their integrated frameworks to primarily study grid impacts of distributed PV combined with demand-side management or district heating networks.

As one contribution of this paper, we take a new perspective of applying integrated building and power system modeling to the task of designing a NZE electrical system with utility ownership and operation of DERs. In the modeling frameworks described above, electrical energy storage has not explicitly been included, but it is key for achieving net zero import on any time resolution less than 1 day by time shifting energy from renewable DERs, particularly PV because it produces power only during daylight hours. This requires new control strategies for the coordinated control of district ESS with hourly or subhourly NZE performance in mind. For example, NZE goals are addressed in Nam et al.,[18] which uses centralized ESS control to smooth a community's net load. More frequently, ESS control within distribution systems has been treated as a profit maximization problem for third-party owners or as a cost and power quality optimization from a utility perspective.[19–21] Extensive work has also been done on ESS operations in islandable microgrids,[22] which extend the NZE idea to complete self-sufficiency; however, most districts occupy the middle ground where islanding is unnecessary and simpler heuristic control methods are valuable to enable NZE design without prohibitive computation.

Additionally, a utility-operated NZE district should proactively address operational challenges, including voltage rise from DERs. Besides classic mechanisms such as load tap changers (LTCs), inverter-interfaced DERs can mitigate voltage rise through reactive power absorption and active power curtailment. A variety of control approaches have been proposed,[23] ranging from central or decentralized optimizations[20,24,25] to local control heuristics, which cannot guarantee global optimum but are easy to implement. Among these, linear piecewise volt/var (VVAR) and volt/watt (VW) droop control will likely receive practical implementation because of the adoption of the newest version of IEEE 1547.[26] Current research is addressing the selection of droop parameters as well as combined VW/VVAR approaches.[27–29]

The contributions of this paper include a novel district control scheme with modified VW/VVAR control for modeling districts aiming to achieve subhourly NZE while mitigating potential grid impacts. This includes a coordinated ESS control scheme that accounts for network losses, storage losses, and available storage capacity. We also develop a highly detailed integrated modeling platform with open-source building and distribution system models. Rather than relying on simplified test systems, stock building profiles, and seasonal weather averages or representative days, this platform performs detailed quasi-static time-series simulations to accurately characterize the impacts of in-district renewable DERs and evaluate grid impacts on actual utility systems.[30] As a case study, the modeling platform is applied to the design of Peña Station NEXT, a new 100-building, 400-acre district on a 1,200-node distribution feeder using actual utility, developer, and weather data at 15-minute resolution from 2016 (35,040 time steps). To focus on the design of the district's DERs, the integrated framework is applied in an exhaustive analysis of the DER design space through 2,551 scenarios to inform the decision process by comparing the scenarios' affordability, self-sufficiency, and grid reliability.

In the remainder of this paper, Section II introduces the three district design objectives, and Section III details the components of the integrated modeling platform. The proposed district DER control scheme is introduced in Section IV. Section V presents the case study on Peña Station NEXT and the results of its multi-objective optimization using the integrated modeling framework; Section VI concludes.

II. NZE DISTRICT DESIGN OBJECTIVES

A NZE district must serve the needs of multiple stakeholders, including its residents and customers, the district developer, and the local utility. In this paper, we apply a multiobjective design process to balance these competing needs by considering the self-sufficiency, investment cost, and reliability of the power system.

The NZE metrics proposed here quantify a district's electrical self-sufficiency and sustainability if using renewable DERs. Although multiple NZE definitions are available,[3] they typically consider a region that can generate as much energy as it consumes over some time hori-

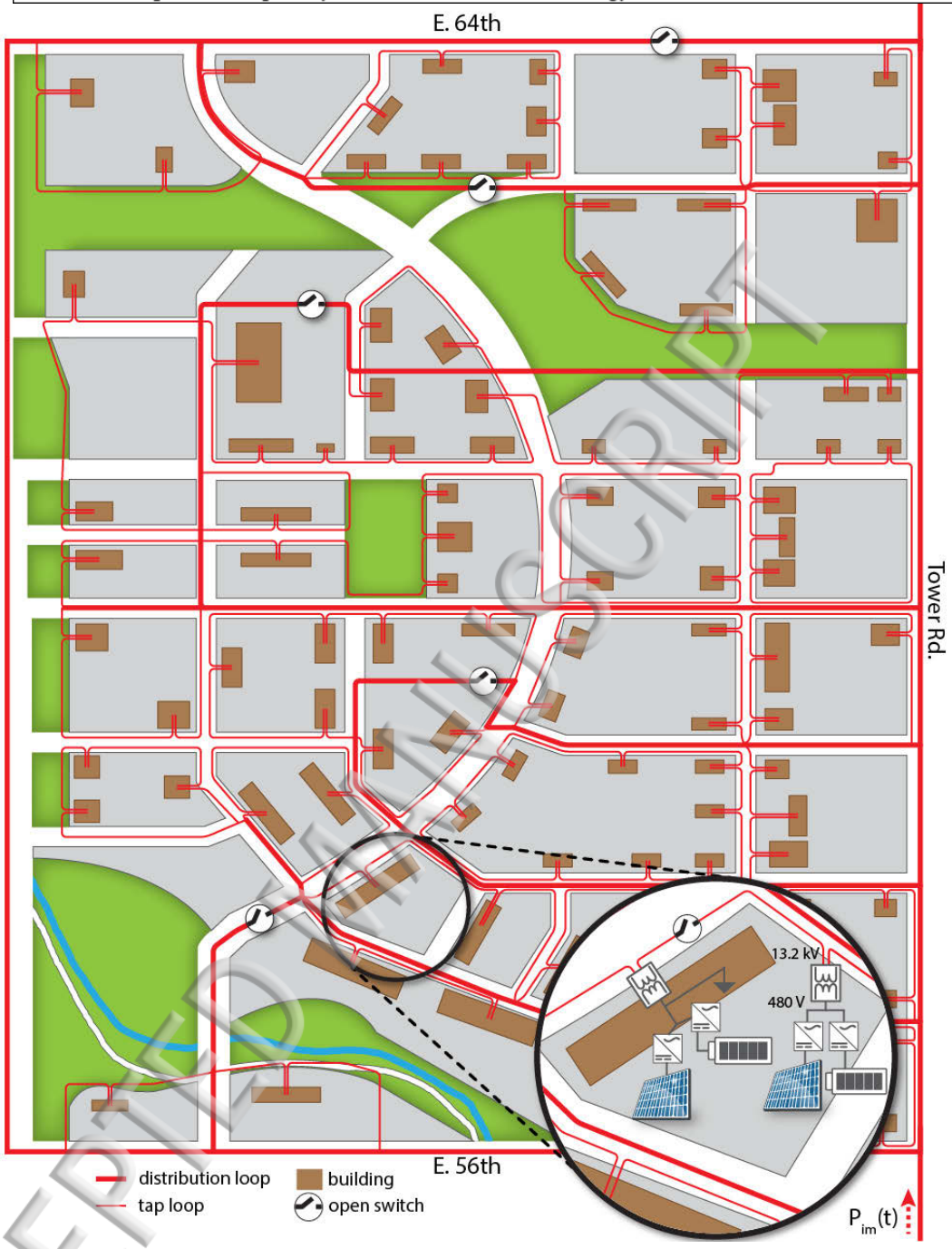

FIG. 1. Peña Station NEXT, including its import power from the distribution feeder, $P_{im}(t)$, and its block, building, and distribution line layout. The inset details one block's building loads, DERs, 13.2-kV-to-480-V transformers, and tap loop open point.

zon to be NZE; however, this obscures losses within the distribution system, renewable curtailment, and other power system impacts important to the utility. Therefore, we define a NZE electrical system as a geographically contiguous portion of a power grid that exports as much electrical energy as it imports during a balancing period. For this accounting, the key value of interest is the district import power, $P_{im}(t)$, which can be calculated by tracking the power flows on the main distribution lines into the district, as shown in Fig. 1 for the case study discussed below. If at a given time the district is generating more power than it is consuming, the district import power will be negative (i.e., it is exporting power).

By tracking the district import power over the course of the annual simulation, two useful NZE metrics can be defined. First, to reflect the fact that NZE communities

commonly assess their own performance over a balancing period of 1 year, we define an annual metric: the annual net energy import (ANEI). ANEI is the sum of the district import energy during the year, where the import energy is approximated by assuming power is constant over the interval of each time step, i.e. at an hourly time step the import energy value (in MWh) would be the same as the import power value (in MW):

$$\text{ANEI (kWh)} = \sum_t T \times P_{im}(t), \tag{1}$$

If the district exports as much energy as it imports over the year, its ANEI will be zero; if it exports more than it imports, ANEI will be negative. Although ANEI is useful in broad strokes, it assumes that the grid can always accommodate the district's power imbalance, obscuring challenges such as backfeeding. Achieving NZE at a finer hourly or subhourly timescale can minimize detrimental impacts, particularly to the utility. As an alternative to ANEI that captures these subhourly imbalances, the cumulative power imbalance (CPI) metric sums the magnitude of the district import power during the year:

$$\text{CPI (kW)} = \sum_t |P_{im}(t)| \tag{2}$$

A district that is balanced at every time point will have zero CPI; otherwise, its CPI will be positive. By considering both annual and sub hourly balancing, implications of the two approaches can be compared.

Next, the DER and transformer initial investment costs for a particular scenario are considered. The DERs in this study are PV and ESS, but other district assets can be included. The turnkey investment cost for commercial PV, $C_{PV,kW}$ ($/kWdc), includes the cost of panels, inverters, and overhead and balance-of-system costs. Distributed ESS are modeled here as Lithium-ion batteries, with costs broken into the battery cost, $C_{ESS,kWh}$ ($/kWh), and the balance-of-system cost, $C_{ESS,kW}$ ($/kW). Therefore, the utility's total investment cost is calculated as:

$$\begin{aligned} C = & C_{PV,kW} * \sum_{i \in B} P_{PV,DC,i} + \sum_{i \in B} C_T(S_{T,i}, X) \\ & + C_{ESS,kWh} * \sum_{i \in B} E_i + C_{ESS,kW} * \sum_{i \in B} S_{ESS,i}. \end{aligned} \tag{3}$$

These investment costs can be used to inform the district's market case. Where known, additional DER operating and lifetime costs can be included, based on the characteristics of the selected technology. For example, where energy storage is implemented with batteries, the storage lifetime costs can include ongoing operating costs, such as maintenance and control software licensing fees, as well as decommissioning and replacement costs.[31] The end-of-life decommissioning costs, which can be significantly higher than the commissioning costs, can be mitigated by second-life uses or salvage.[31] It is important to note that frequent battery cycling for energy-time shifting, as applied in this case study, can lead to faster battery degradation and a shorter battery lifespan,[32] increasing the frequency of capital reinvestment.

In this instance, it is assumed the utility would own and operate the DERs within the district, so it might be appropriate to also include system operations and maintenance costs. For example, some service territories have historically used LTCs for voltage control, which may incur more frequent tapping due to variable DER generation, resulting in increased wear and decreased life expectancy. These costs could also be included in (3), though it should be noted that access to time-series data at a much finer resolution (seconds rather than minutes) is likely required to fully assess tapping impacts.[30] In the case study below, there are no capacitor banks or LTCs beyond the substation, so these costs are omitted.

For simplicity, (3) also does not include the marginal build-out of the utility's supervisory control and data acquisition (SCADA) system to enable visibility of the district's power system, including the power flows in and out of the district required to assess the net power import, $P_{im}(t)$. It is assumed these costs are absorbed by the utility and would be incorporated into the district's rate-case once the design is finalized.

Finally, system performance is assessed by the annual sum of line ampacity and node under- and overvoltage violations:

$$\mathcal{V} = \sum_t \left(\mathcal{V}_{amp}(t) + \mathcal{V}_{UV}(t) + \mathcal{V}_{OV}(t) \right). \tag{4}$$

This provides a sense of the system reliability and viability to inform the design process. Once a particular design has been selected, additional DER operational optimizations can be performed to fine-tune performance (e.g., Fortenbacher et al.[33]).

Together, these objectives can be used to compare district scenarios to ensure that the district developer can achieve its self-sufficiency goals, the utility can operate the system reliably, and the costs passed down to customers are affordable.

III. INTEGRATED LOAD AND GENERATION MODEL

To assess these multiple objectives for different district scenarios, a simulation framework integrating open-source tools is developed to endogenously model buildings, DERs, and the distribution system. Fig. 2 shows the simulation block diagram, and Fig. 1 illustrates the model components for the Peña Station NEXT case study. First, the individual buildings within the district are modeled in URBANopt,[34] a district-level modeling tool developed on top of OpenStudio.[35,36] The main advantage of using URBANopt over a more detailed building energy modeling tool such as BEopt[37] or OpenStudio is that the level of input detail required by URBANopt

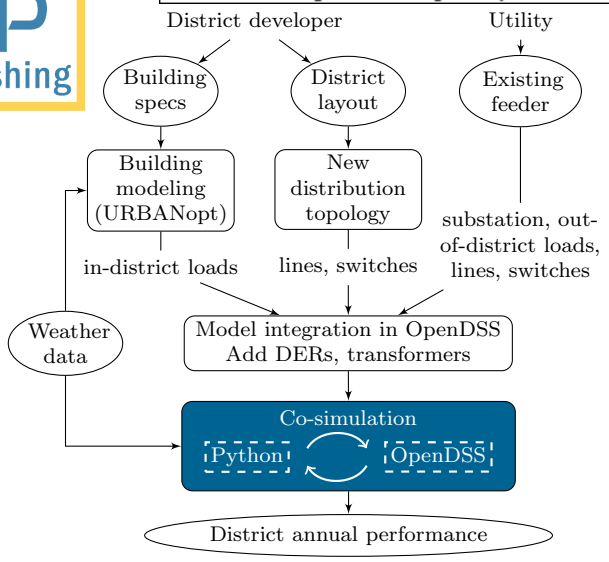

FIG. 2. Block diagram of integrated district simulation framework, including buildings modeling in URBANopt leading into Python/OpenDSS distribution system cosimulation.

matches what is typically available early in the design process, while the other tools require much more detailed input. Inputs received from the district developer are each building's square footage, height, and use type.

A variety of demand-side technologies can be incorporated into URBANopt, such as higher insulation, all-LED lighting, or advanced ventilation systems. Based on the developer inputs, technology selection, and local weather data, each building's electrical load is simulated at 15-minute resolution over 1 year. One important note is that URBANopt does not model reactive power, necessitating assumptions about power factor to develop a complete load model; in this case study, a constant 0.95 inductive power factor was assumed. While the endogenous load modeling is key to detailed design of the district rather than relying on stock building profiles, the remainder of the paper will put more focus on the DER sizing and operational strategy. For more information on building energy modeling itself, the interested reader is referred to Reinhart et al.[38] and the references therein.

Once modeled in URBANopt, the building electrical loads are exported into OpenDSS.[39] There are several options for proprietary or open-source distribution system power flow solvers, of which OpenDSS and GridLAB-D are well-known open-source options that are free to the public.[40] OpenDSS can support a variety of frequency domain analyses for distribution systems, including solving the unbalanced 3-phase power flow for the system's RMS steady-state values. Therefore, it can employed for "quasi-static" time-series simulations by solving the power flow at each time step – in this instance, by acting as a "black-box" solver to find the RMS solution at each of the 35,040 time steps. OpenDSS has the added benefit that it can be interfaced with other programs through its built-in COM interface or through one of the "OpenDSSDirect" Python or Julia packages to implement customized models or controls.

To incorporate DERs into the OpenDSS model, rooftop PV is added to each building and car canopy or ground-mounted PV to each city block; ESS are connected at each of these locations as well (Fig. 1 inset). A PV system's time-varying inverter output is modeled endogenously in OpenDSS based on the same weather data used in the building models, according to:

$$P_{PV,i}(t) = \min\left\{ P_{PV,DC,i} \frac{I(t)}{1\text{kW/m}^2} \eta_{inv} \eta_{PV}\left(\mathcal{T}(t)\right), \; S_{PV,i} \right\} \quad (5)$$

In the case study below, the weather-dependent module temperature $\mathcal{T}(t)$ is simulated in SAM[41] for a typical fixed roof-mounted commercial system with 20° tilt, and the temperature-dependent efficiency $\eta_{PV}\left(\mathcal{T}(t)\right)$ is estimated for a typical Sunpower module. ESS operation during the course of the year is addressed in Section IV A. Determining the appropriate capacity of PV and ESS installations to balance the trade-off between investment costs and district self-sufficiency is one of the major design questions at hand, addressed in Section V C.

At each building or block site, the load, PV, and ESS will connect to the distribution system through a 13.2-kV-to-480-V three-phase transformer. Each transformer is sized according to:

$$S_{T,i} = \chi\left(\max\left\{\overline{P_{load,i}}, S_{PV,i} + S_{ESS,i} \quad , X\right\}\right), \quad (6)$$

where χ is a look-up function that selects a transformer from the utility's catalog to ensure that its kVA rating minimally exceeds the maximum of the building peak load and the sum of the PV and ESS inverter ratings.

Next, medium-voltage (13.2-kV) distribution lines are modeled from the new district assets to interconnect with the existing distribution feeder. Based on the layout determined by the district developer, new distribution lines are delineated according to utility practice (Fig. 1). "Tap loops" connect the transformers around each block with low-ampacity lines. High-ampacity "distribution loops" connect multiple tap loops back to the existing distribution feeder. Line impedances and ampacities are provided by the utility's proprietary hardware catalog. As indicated in the detailed figure inset, each of these physical loops contains an open switch, and it is not operated as an electrical loop. As with the building models, the distribution topology is exported into OpenDSS.

In addition to the district elements, the existing feeder and its loads are added to the model, bringing the total size to 1,200 nodes. The feeder loads are modeled with time-synchronous load data from the same year as the weather data used in the district load and PV models. These existing loads and feeder lines are modeled using recorded utility data, but are not illustrated here due to privacy concerns. Including them allows for holistic simulation of the district's interactions with the surrounding neighborhoods and impacts at the substation level.

Once these components are all synthesized in one model in OpenDSS, the district's operation is evaluated at subhourly resolution over 1 year by cosimulating with customized controls implemented in Python, detailed next.

IV. DISTRICT CONTROL ALGORITHM

Within the modeling framework, a new control algorithm is required to model the particular behavior of a NZE district. To pursue NZE on a subhourly basis, a centralized, coordinated control scheme for district DERs is developed. It is assumed that perfect load and PV forecasts are available; battery state of charge (SOC) can be accurately estimated; DERs are operated by the utility; and a SCADA system monitors the distribution lines entering the district and communicates with local controllers at each building and block interconnection. Given the multiobjective focus, a heuristic control algorithm is developed to balance the NZE objective with grid stability requirements. The control scheme is intended to emulate the desired behavior for a wide range of scenarios; once likely district designs are selected, further operational optimizations can refine performance.

The control scheme, implemented for each time point in the annual simulation, is illustrated in Fig. 3. An initial power flow is run in OpenDSS to select the substation LTC position to maintain 1.05 p.u. voltage on its secondary side. ESS powers are iteratively resolved to smooth the district's net load and achieve zero power import, if possible. PV VW/VVAR control is then iteratively converged to minimize remaining overvoltage issues; the iteration simulates stepping through inverters "hunting" along their voltage control droop curves in search of the steady state operating point.[42] The control scheme is implemented in Python, with the impacts of each decision assessed by rerunning the OpenDSS power flow. ESS and PV control phases are detailed below.

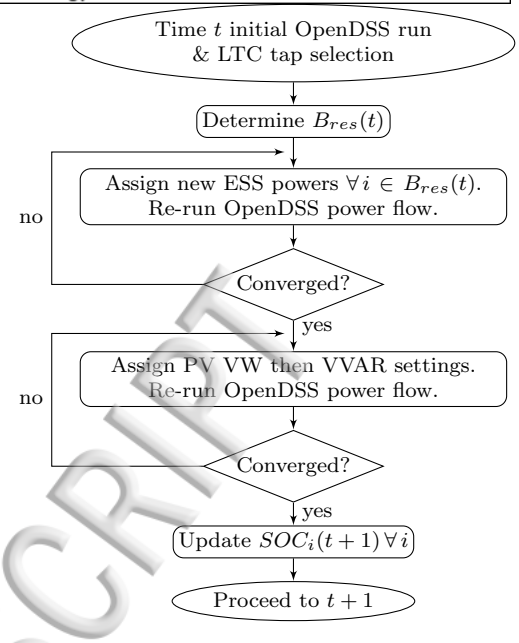

FIG. 3. Control scheme of in-district DER assets at each time-point.

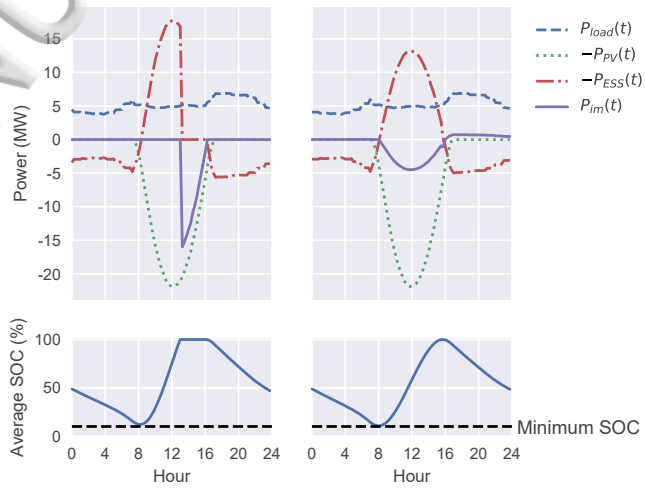

FIG. 4. Impact of ESS control strategy on district power import without (left) and with (right) a forecasted look-ahead.

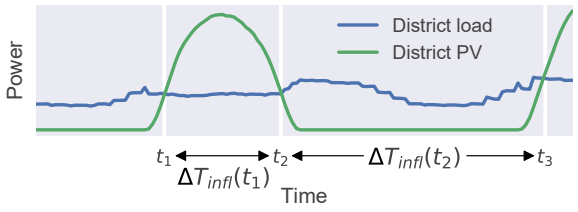

FIG. 5. Inflection time points are identified to help smooth ESS (dis)charging behavior, given the anticipated load and generation imbalance during the time interval to the next inflection point.

A. ESS Energy Time-Shifting

For a NZE district with only PV generation, the primary objective of ESS is to time-shift PV energy from day to night to even out the district's load throughout time, ideally achieving zero CPI; however, undesirable behavior occurs if the controller simply tries to minimize the district power import $P_{im}(t)$ at each time point regardless of current ESS SOC and future conditions. For instance, in Fig. 4, ESS charge with excess PV power until reaching maximum SOC, causing a large spike in uncurtailed power exported from the district. Achieving zero power import in the short term results in more erratic behavior, increased reverse power flows, and increased likelihood of ampacity and voltage violations in the long term.

This behavior is improved by using load and PV forecasts, from which inflection points can be determined, as shown in Fig. 5. When district load rises above PV generation (and vice versa), ESS should switch from charging to discharging (and vice versa) to achieve the ideal zero power import; however, ESS might not have sufficient energy to supply district load until the next inflection point (or sufficient headroom to charge all excess PV power). Therefore, a look-ahead damping factor, $\lambda(t)$, is calculated at each inflection point to smooth (dis)charging behavior until the next inflection. ESS charging is slowed to a fraction of the ideal power with the goal of reaching the SOC limit just at the next inflection point. As demonstrated in Fig. 4, this approach smooths ESS behavior by sacrificing some zero import performance in the short-term to mitigate undesirable grid impacts. Given this trade-off, a goal of the multiobjective scenario analysis is to determine adequate DER capacities to minimize the impact of the look-ahead and maintain zero import as much as possible.

This ESS control algorithm is executed as follows. The forecasted energy imbalance from time t to the next inflection point is calculated from (5) and the building load profiles as:

$$E_{im}(t) = \left| \sum_{\tau=t}^{t+\Delta T_{infl}(t)} \left(P_{PV}(\tau) - P_{load}(\tau)\right) \right|. \quad (7)$$

The upward and downward ESS energy capacities are calculated, respectively, as:

$$E_{up}(t) = \sum_{i \in B} \sqrt{\eta_{RT}} E_i \frac{\left(\overline{SOC} - SOC_i(t)\right)}{100}, \quad (8)$$

$$E_{down}(t) = \sum_{i \in B} \sqrt{\eta_{RT}} E_i \frac{\left(SOC_i(t) - \underline{SOC}\right)}{100}. \quad (9)$$

These energy capacities account for SOC limits and inverter round-trip efficiency losses indicative of a utility-scale Li-ion battery. Depending on the ESS system, (8)-(9) can be modified to account for other losses, such as energy siphoned for temperature maintenance and low-voltage battery monitoring, control, and safety systems.[31]

If the time is an inflection point, a new look-ahead damping factor is calculated from (7)-(9); otherwise, it remains the same:

$$\lambda(t) = \begin{cases} \min\left\{\frac{E_{up}(t)}{\rho E_{im}(t)}, 1\right\}, & \text{if } P_{load}(t-1) \geq P_{PV}(t-1) \text{ and } P_{load}(t) < P_{PV}(t) \\ \min\left\{\frac{E_{im}(t)}{\rho E_{down}(t)}, 1\right\}, & \text{if } P_{PV}(t-1) \geq P_{load}(t-1) \text{ and } P_{PV}(t) < P_{load}(t) \\ \lambda(t-1), & \text{otherwise} \end{cases} \quad (10)$$

An optional uncertainty factor, ρ, can be added as a conservative measure to account for both forecasting errors and distribution system losses that are not included in (7). Note that the case study below assumes a perfect forecast; the impact of forecast errors on system design and sensitivity to selection of ρ are left for future work.

Next, an initial OpenDSS power flow is run with all PV systems generating at their maximum power points to determine the district power import. Given current ESS SOCs, only some systems might be able to (dis)charge as needed to reduce the power import to zero. The responsive subset is defined as:

$$B_{res}(t) = \begin{cases} \{i \in B \,|\, SOC_i(t) > \underline{SOC}\}, & P_{im}(t) \geq 0 \\ \{i \in B \,|\, SOC_i(t) < \overline{SOC}\}, & \text{otherwise} \end{cases} \quad (11)$$

That is, when the district would be importing power, the responsive ESS must have stored energy to discharge to replace import power. Conversely, when the district would be exporting, responsive ESS must have headroom to absorb some of the excess.

Next, the central controller enters an iterative loop to adjust the responsive ESS (dis)charge powers until convergence is reached. Iterative convergence is required because the ESS power needed to achieve zero instantaneous import does not equal the difference of load and generation because of distribution system losses. At each iteration j through the control loop at time t, the ideal new output power of each responsive ESS is calculated from its share of the previous district import power:

$$P_{new,i}(t,j) = P_{ESS,i}(t,j-1) + P_{im}(t,j) \frac{S_{ESS,i}}{\sum_{i \in B_{res}(t)} S_{ESS,i}} \quad (12)$$

Each responsive ESS is updated with the desired output power, constrained by its inverter rating:

$$P_{ESS,i}(t,j) = \lambda(t) \min\left\{\max\left\{-S_{ESS,i}, P_{new,i}(t,j)\right\}, S_{ESS,i}\right\} \quad \forall\, i \in B_{res}(t) \quad (13)$$

The remaining ESS that do not have the SOC capacity to respond always have zero power (i.e., $P_{ESS,i}(t,j) =$

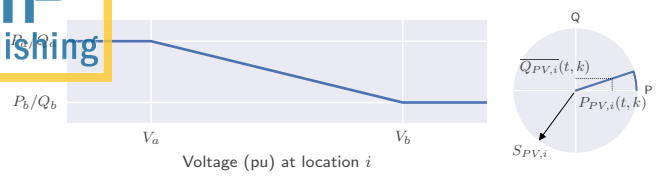

(a) (b)

FIG. 6. (a) Piecewise linear VW\VVAR droop curve. (b) Maximum reactive power for VVAR is limited by power factor and inverter rating.

TABLE I. Voltage Droop Parameters

	$P_a \backslash Q_a$	$P_b \backslash Q_b$	V_a (pu)	V_b (pu)
VW	$P_{PV,i}(t,0)$	$\max\{-P^*_{ESS,i}(t), 0\}$	1.05	1.10
VVAR	0	$-\overline{Q_{PV,i}}(t,k)$	1.00	1.10

$0 \; \forall \; i \notin B_{res}(t) \; \forall \; j$). The OpenDSS simulation is then rerun to assess the impact of the new set points on the district power import.

Convergence may be reached in two ways. First, it may be determined that the district is supplying all its own power if power crossing the district boundaries is near to zero, within a NZE tolerance:

$$|P_{im}(t,j)| < \varepsilon_Z \tag{14}$$

Alternatively, the district import may have reached a nonzero steady state because of the look-ahead damping factor or ESS power ratings, where change between iterations is within a small value;

$$|P_{im}(t,j) - P_{im}(t,j-1)| < \varepsilon_C \tag{15}$$

Last, the SOC is updated according to (16), constrained to ensure $\underline{SOC} \leq SOC_i(t+1) \leq \overline{SOC}$, where $SOC_i(1) = 50\% \, \forall \, i$.

$$SOC_i(t+1) = SOC_i(t) - \frac{\psi P^*_{ESS,i}(t) T}{E_i} \times 100, \tag{16}$$

$$\text{where } \psi = \begin{cases} \sqrt{\eta_{RT}}, & \text{if } P^*_{ESS,i}(t) < 0 \text{ (i.e., charging)} \\ \frac{1}{\sqrt{\eta_{RT}}}, & \text{otherwise} \end{cases}$$

The asterisk indicates final values from the control loop.

B. PV Voltage Control

Once ESS powers are selected, PV voltage control is added in a second iterative loop. A controller at each PV/ESS pair monitors the local voltage, $V_i(t)$, and applies first VW and then VVAR control. Fig 6(a) illustrates the linear piecewise droop curve, where the a and b subscripts denote parameters at the lower and upper voltage thresholds, respectively. Table I reports the corresponding droop parameters, based on industry standards in IEEE Standard 1547-2018;[26] however, to customize the VW control for a NZE district, PV generation is curtailed no further than the charging level of its ESS pair to avoid interference with the selected set points. Therefore, the VW equation for iteration k at time t if $V_{a,VW} < V_i(t,k-1) < V_{b,VW}$ is:

$$P_{PV,i}(t,k) = P_{PV,i}(t,0) - m_i(t) \left[V_i(t,k-1) - V_{a,VW} \right] \tag{17}$$

where $P_{PV,i}(t,0)$ is the uncurtailed power and the slope is:

$$m_i(t) = \frac{P_{PV,i}(t,0) - \max\left\{0, -P^*_{ESS,i}(t)\right.}{V_{b,VW} - V_{a,VW}} \tag{18}$$

Next, each smart inverter implements VVAR control as:

$$Q_{PV,i}(t,k) = -\overline{Q_{PV,i}}(t,k) \frac{(V_i(t,k-1) - V_{a,VVAR})}{(V_{b,VVAR} - V_{a,VVAR})}, \tag{19}$$

if $V_{a,VVAR} < V_i(t,k-1) < V_{b,VVAR}$. The maximum allowable reactive power, $\overline{Q_{PV,i}}(t,k)$, is limited by a 0.97 power factor, as illustrated in Fig. 6(b), to avoid excessive reactive power absorption in scenarios with high capacities of installed PV. This algorithm focuses on mitigating overvoltages from DERs in close urban districts where voltage drops along the feeder are small but undervoltage VAR support can be similarly applied. The VW-VVAR logic is iterated until the average voltage change at the DER locations converges within a voltage tolerance:

$$\frac{\sum_{i \in B} |V_i(t,k-1) - V_i(t,k)|}{|B|} < \varepsilon_V. \tag{20}$$

V. CASE STUDY: PEÑA STATION NEXT

As a case study, the simulation framework is applied to design Peña Station NEXT (PSN), a developing 100-building, 400-acre mixed-use urban district in Denver, Colorado, for which solar PV is the primary local renewable resource of interest.

A. URBANopt Building Simulations

The new development is planned to comprise 6 low- and 39 high-density residential buildings, 3 hotels, 26 offices, 11 full and quick-service restaurants, and 8 stand-alone and 10 strip-mall stores. Based on the developer's specifications, the electrical load of each building is simulated in URBANopt at 15-minute resolution (i.e., $T = 0.25$ h) with 2016 weather data recorded near the development. Two efficiency scenarios are considered: a baseline compliant with ASHRAE 90.1-2013 building

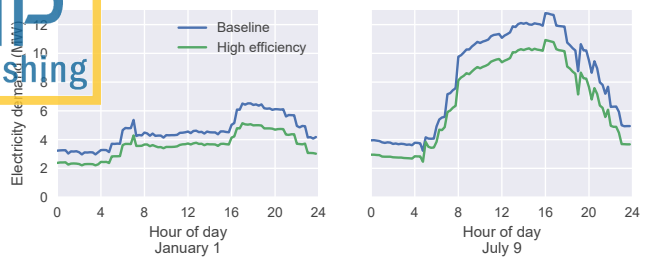

FIG. 7. Total district electricity use is reduced by high efficiency measures, illustrated for (left) January 1 and (right) the peak load day, July 9.

code[43] and a high-efficiency case, which includes reduced infiltration and plug load, increased insulation, all-LED lighting, increased effectiveness energy-recovery ventilators, and smart outdoor lighting controls. The high efficiency case reduces annual electricity demand by 20% from 52.0 GWh to 41.5 GWh, with significant reduction of daily and annual peak loads, as shown in Fig. 7. Given its significant impact on electric load, the multiobjective DER scenario analysis performed next is demonstrated with the high efficiency building scenario.

B. Power System Description and DER Scenarios

The proposed distribution system serving PSN is illustrated in Fig. 1 and interconnected with a proprietary model of the local distribution feeder extending to the nearest substation, provided by Xcel Energy. Out-of-district loads in the surrounding neighborhoods are modeled with a time-synchronous 2016 load profile measured at the feeder substation. The power system model including PSN comprises ~1,200 nodes.

For the high efficiency building scenario, a host of DER scenarios are considered to evaluate the multiple objectives in Section II. To calculate investment costs, Li-ion battery costs from 2015[31] and turnkey PV costs from 2017[44] are used. Although battery costs have dropped significantly in the last few years, this will change the magnitude but not the trends of the results. The maximum PV capacity at each building and city block is geographically constrained by the rooftop and car canopy area. Fifty percent of the building area is allocated for rooftop PV with an industry typical fill factor of 18 W/ft^2, assuming 20% efficient PV panels. Forty percent of the remaining area on the city blocks is allocated for car canopy and ground-mounted installations, with a fill factor of 0.2 MW/acre.

The maximum ESS capacity at each location is proportional to its PV capacity, so the total allowable in-district energy capacity is 500 MWh. This capacity is selected to determine if the district can achieve 15-minute NZE during the period of lowest PV generation, a 3-day clouded period in winter during which the total in-district load is ~430 MWh. For this case study, ESS is applied only for energy time-shifting, but it can also be used for a variety of other services, such as voltage regulation, frequency regulation, or primary contingency reserves. If desired, a fixed capacity can be held in reserve for these other services and the ESS capacity expanded accordingly. This changes the magnitude but not the relative difference in ESS capacity among scenarios considered here.

TABLE II. Case Study Simulation Parameters

η_{RT}	η_{inv}	$\underline{SOC}$	$\overline{SOC}$	ρ	ε_Z	ε_C	ε_V
85.5%	98.4%	10%	100%	3%	10 kW	2 kW	0.005 pu

As an exhaustive search of the design space within the maximum DER capacity limits, 2,551 scenarios are evaluated with differing proportions of PV and storage from 0% to 100% of their maximum capacities, in increments of 2%. Scenarios with storage but no PV are ignored. For each scenario, PV inverters are rated with a DC-to-AC ratio of 1.2 (i.e., $S_{PV,i} = \frac{P_{PV,DC,i}}{1.2\ \text{kWdc}}$kVA), and the ESS inverters are rated with a 2:1 energy-to-power ratio (i.e., $S_{ESS,i} = \frac{E_i}{2\ \text{kWh}}$kVA). It is important to note again that while the power flow equations were not enumerated in the sections above, the 3-phase RMS power flow is being solved within OpenDSS, given the DER power injections, load powers, and impedances of the ~1,000 distribution lines within the feeder. Given the "black-box" characteristic of OpenDSS, future work may consider a "sim-opt" approach to optimize the lay-out of DER assets in the district,[45] but the exhaustive search approach can also by applied to illustrate the trade-offs within the design space.

The 2,551 scenarios were run in parallel on Peregrine, the National Renewable Energy Laboratory's (NREL) high-performance computing system. Simulation parameters are given in Table II. Through these scenarios, trade-offs among the three key objectives – investment cost, total violations, and CPI – can be determined, and additional metrics can be evaluated, such as ANEI and PV curtailment.

C. Multiobjective DER Scenario Analysis Results

Figs. 8 to 11 show comparisons of the 2,551 DER scenarios, 10 of which did not converge in the time allotted, and highlight four scenarios, including the no-DER baseline. When comparing multiple objectives, a Pareto front can be found as the set of nondominated solutions, or those that cannot be improved in one objective without their performance deteriorating in at least one other metric. In this case, the 3-dimensional Pareto front is determined by investment cost, total violations, and CPI. In these figures, the dominated solutions are represented as tan dots, while the non-dominated solutions on the Pareto front are highlighted in blue.

As is expected, increasing PV capacity decreases the

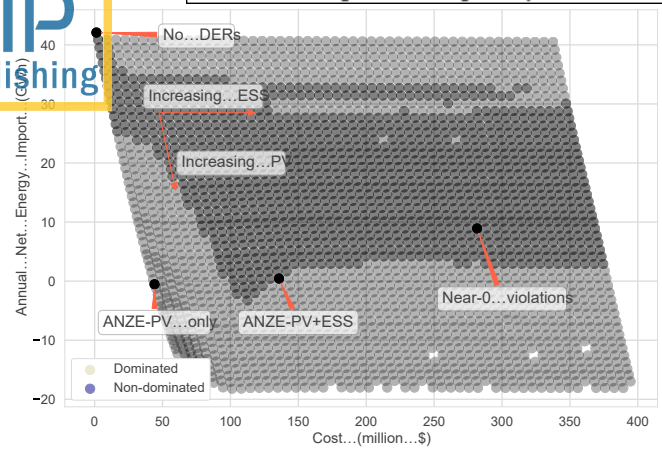

FIG. 8. Annual NZE, indicated by zero ANEI, is reached with ∼27 MW of installed PV. With higher PV installations, the district has net positive energy.

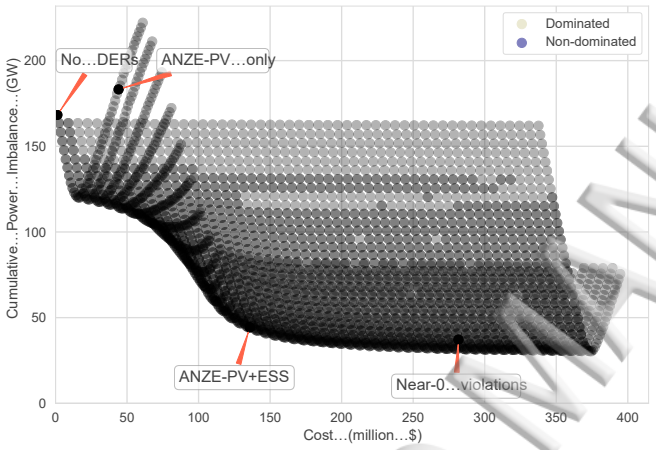

FIG. 9. 15-minute NZE, corresponding to zero CPI, is not achieved for the DER scenarios considered here, but significant improvement can be made by adding battery storage for intraday energy time-shifting.

annual net energy import, eventually resulting in net-positive energy solutions as shown in in Fig. 8. However, as the ANEI metric is insensitive to the timing of energy generation and consumption, the time-shifting action of ESS has no impact from this perspective. In contrast, when considering the 15-minute time-scale, increasing PV capacity up to ∼9 MW decreases CPI, but beyond that point, curtailment and power backfeeding deteriorate performance (Figs. 9-10). For these scenarios with higher PV penetrations, adding ESS capacity to time-shift energy improves 15-minute NZE performance by reducing backfeeding and lowering the power import at times of low generation.

The four highlighted scenarios help illustrate these general trends. With PV alone, annual NZE is nominally achieved with 27.3 MW PV, shown by the ANZE-PV only scenario; however, when considering 15-minute NZE

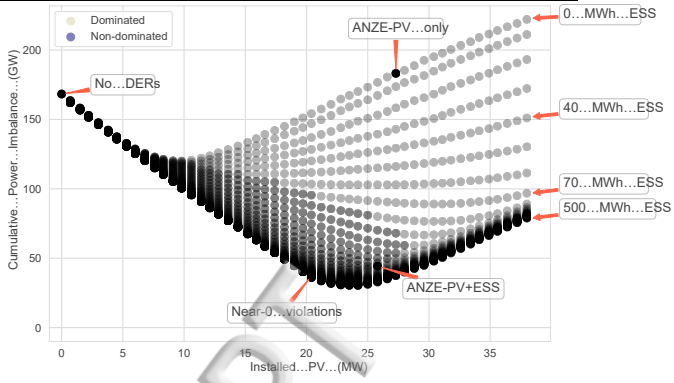

FIG. 10. CPI decreases with increasing PV penetration, up to a point where curtailment and power backfeeding deteriorate performance.

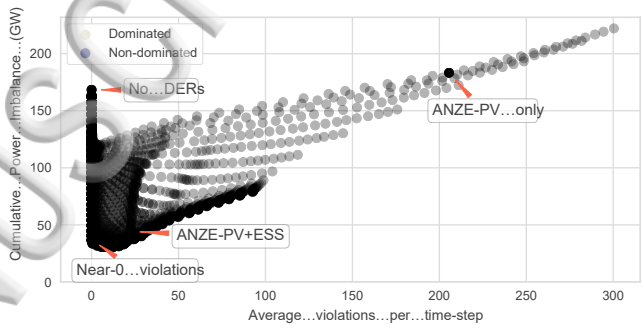

FIG. 11. Scenarios with excessive power export due to power backfeeding are associated with a large number of average operational violations per time step.

(Fig. 9), the ANZE-PV only scenario performs poorly due to backfeeding. To consider the benefits of adding ESS, the ANZE-PV+ESS scenario, which has 25.8 MW of PV and 140 MWh of ESS, also achieves annual NZE, but reduces CPI 76% compared to ANZE-PV only.

Together with power backfeeding, the ANZE-PV only scenario suffers from frequent operating violations. Fig. 11 shows the average operational violations per time steps, with voltage violations counted for the 1,173 nodes and ampacity violations for the 1,018 lines. By reducing backfeeding through energy time-shifting, the ANZE-PV+ESS scenario reduces violations by 89% compared to the ANZE-PV only scenario. However, scenarios with significant violations are infeasible in practice, so it is valuable to instead determine how close the district can get to NZE without violations. In answer, the "near-0 violations" scenario is that with the lowest ANEI and CPI without significant violations. It reduces both ANEI and CPI ∼78% compared to the baseline, but it incurs more than double the capital cost of the ANZE PV+ESS scenario. On the other hand, the voltage control scheme is intended to reduce but not eliminate violations; control refinement could further reduce violations once likely lower cost scenarios are selected.

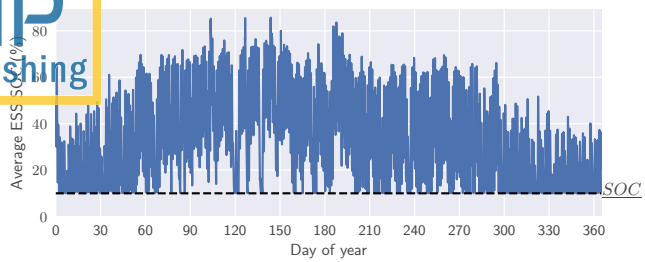

FIG. 12. ANZE-PV+ESS scenario average ESS SOC, indicating the need for seasonal storage to shift summer excess PV energy to serve winter loads.

Notably, the district does not achieve zero CPI (15-minute NZE), even with extensive storage. In this analysis, ESS is operated only for intraday energy shifting. Ideally, its SOC should fluctuate from one day to the next in the mid-range without hitting its minimum or maximum limits; however, as illustrated in Fig. 12 for the ANZE-PV+ESS scenario, the average ESS SOC $\left(\frac{\sum_{i\in B} SOC_i(t)}{|B|}\right)$ shows seasonal variability, reflecting the availability of ample PV generation in summer but reduced output in winter. With only intraday shifting, ESS does not effectively address seasonal fluctuations. To avoid overbuilding PV to boost winter generation, districts with limited generation options could consider added storage for seasonal energy shifting, though applicable technologies (e.g., compressed air energy storage, pumped hydro) are more feasible for NZE cities or regions than districts. Technologies appropriate for districts (e.g., hydrogen fuel cells, flow batteries) are promising but still developing. Alternatively, the district could benefit from diversifying its generation with wind, microhydro, and/or biogas, if available. Other URBANopt building scenarios could also be assessed to compare more extensive DER buildouts to more advanced building measures, such as seasonal thermal storage, to bridge to gap to zero CPI.

VI. CONCLUSIONS

This paper develops an integrated building and power system model for designing districts with very high renewable energy penetrations, with an eye towards achieving net zero energy. In this framework, impacts of both demand-side and supply-side technologies on the district's affordability, self-sufficiency, and power system reliability can be assessed. The framework includes a new bilevel control model to manage the district's net power import and voltage rise from high distributed PV penetrations with both central and local control of DERs. This control model assumes DERs can be operated by the utility, but the framework can easily be extended to other ownership and operation scenarios, including private-owned DERs or a combination of private and utility ownership.

The control scheme presented here is intended to facilitate district design based on time-series data to capture the impacts of variable renewable generation, in contrast with classic distribution system design that relies solely on the anticipated peak loads. In general, such time-series studies should rely on the finest resolution time-series data available. In the case study here, 15-minute data is used to capture subhourly power imbalances, though this resolution still obscures high frequency solar variation at the seconds and minutes time-scale. Once likely designs are selected, they should be subjected to further dynamics and operational analysis, including sensitivity to whatever actual load and weather forecasts are available, in contrast with the perfect forecast assumed here.

As a case study, the framework is applied to design a new urban district – Peña Station NEXT – to illustrate the costs of achieving varying DER penetrations, up to and including annual NZE; however, the district, which has only PV generation available, is limited by seasonal fluctuations in PV output and cannot achieve NZE on a 15-minute basis, highlighting the need for seasonal electric and/or thermal storage. It is important to note that the present case study puts more emphasis on the DER build-out and distribution system modeling, leaving opportunity for more coordination with the buildings themselves through the building automation systems (BAS). For future work, the power system state can be fed back into URBANopt for coordinated building and power system controls, including demand response with thermal comfort constraints. The modeling platform can also be extended to consider other impacts on the district design, including seasonal storage, heating electrification, and electric vehicle charging. The modeling framework can be similarly applied to district retrofits and sustainable city planning to balance the various needs and goals of the stakeholders, including the municipality, customers, land developer, and utility.

ACKNOWLEDGMENTS

The authors would like to thank Adarsh Nagarajan, Anthony Florita, & Tarek Elgindy (NREL); Chad Nickell & Beth Chacon (Xcel); Mike Hess, Peter Jacobson, & Yun Lee (Panasonic); Rick Wells & Blake Fulenwider (Fulenwider); and the rest of the PSN team, as well as Billy Roberts for their contributions.

This work was authored by Alliance for Sustainable Energy, LLC, the Manager and Operator of the National Renewable Energy Laboratory for the U.S. Department of Energy (DOE) under Contract No. DE-AC36-08GO28308. The views expressed in the article do not necessarily represent the views of the DOE or the U.S. Government. The U.S. Government retains and the publisher, by accepting the article for publication, acknowledges that the U.S. Government retains a nonexclusive,

[1] S. Joss, R. Cowley, and D. Tomozeiu, "Towards the ubiquitous eco-city: an analysis of the internationalisation of eco-city policy and practice," Urban Research & Practice **6**, 54–74 (2013).

[2] A.-F. Marique and S. Reiter, "A simplified framework to assess the feasibility of zero-energy at the neighbourhood/community scale," Energy and Buildings **82**, 114–122 (2014).

[3] S. Koutra, V. Becue, M.-A. Gallas, and C. S. Ioakimidis, "Towards the development of a net-zero energy district evaluation approach: A review of sustainable approaches and assessment tools," Sustainable Cities and Society **39**, 784–800 (2018).

[4] S. Zaleski, S. Pless, and B. J. Polly, "Communities of the future: Accelerating zero energy district master planning: Preprint," Tech. Rep. NREL/CP-5500-71841 (National Renewable Energy Laboratory, Golden, CO (United States), 2018).

[5] J. Allegrini, K. Orehounig, G. Mavromatidis, F. Ruesch, V. Dorer, and R. Evins, "A review of modelling approaches and tools for the simulation of district-scale energy systems," Renewable and Sustainable Energy Reviews **52**, 1391–1404 (2015).

[6] R. A. Lopes, J. Martins, D. Aelenei, and C. P. Lima, "A cooperative net zero energy community to improve load matching," Renewable Energy **93**, 1–13 (2016).

[7] R. E. Best, F. Flager, and M. D. Lepech, "Modeling and optimization of building mix and energy supply technology for urban districts," Applied Energy **159**, 161–177 (2015).

[8] R. Baetens, R. De Coninck, J. Van Roy, B. Verbruggen, J. Driesen, L. Helsen, and D. Saelens, "Assessing electrical bottlenecks at feeder level for residential net zero-energy buildings by integrated system simulation," Applied Energy **96**, 74–83 (2012).

[9] A. Gahran, "2018 state of the electric utility survey," Tech. Rep. (Utility Dive, 2018) `https://www.utilitydive.com/library/2018-state-of-the-electric-utility-survey-report/`.

[10] "Xcel Energy aims for zero-carbon electricity by 2050," `https://www.xcelenergy.com/company/media_room/news_releases/xcel_energy_aims_for_zero-carbon_electricity_by_2050`.

[11] B. Morvaj, R. Evins, and J. Carmeliet, "Optimization framework for distributed energy systems with integrated electrical grid constraints," Applied Energy **171**, 296–313 (2016).

[12] B. Morvaj, R. Evins, and J. Carmeliet, "Decarbonizing the electricity grid: The impact on urban energy systems, distribution grids and district heating potential," Applied Energy **191**, 125–140 (2017).

[13] C. Molitor, S. Groß, J. Zeitz, and A. Monti, "MESCOS–a multi-energy system cosimulator for city district energy systems," IEEE Transactions on Industrial Informatics **10**, 2247–2256 (2014).

[14] K. Kusakiyo, Y. Yamaguchi, and Y. Shimoda, "Community-scale residential energy demand simulation for smart-grid applications," in *Proceedings of the 13th Conference of International Building Performance Simulation Association* (Chambéry, France, 2013) pp. 2725–2732.

[15] T. Fujimoto, Y. Yamaguchi, and Y. Shimoda, "Energy management for voltage control in a net-zero energy house community considering appliance operation constraints and variety of households," Energy and Buildings **147**, 188–199 (2017).

[16] R. De Coninck, R. Baetens, D. Saelens, A. Woyte, and L. Helsen, "Rule-based demand-side management of domestic hot water production with heat pumps in zero energy neighbourhoods," Journal of Building Performance Simulation **7**, 271–288 (2014).

[17] C. Protopapadaki and D. Saelens, "Heat pump and PV impact on residential low-voltage distribution grids as a function of building and district properties," Applied Energy **192**, 268–281 (2017).

[18] H.-S. Nam, S.-J. Lee, T.-H. Kim, Y.-K. Hong, and Y.-K. Jeong, "Optimization mechanism of energy cluster for zero energy town," in *2017 International Conference on Information and Communication Technology Convergence (ICTC)* (Jeju, South Korea, 2017) pp. 1121–1123.

[19] M. Nick, R. Cherkaoui, and M. Paolone, "Optimal allocation of dispersed energy storage systems in active distribution networks for energy balance and grid support," IEEE Transactions on Power Systems **29**, 2300–2310 (2014).

[20] R. Zafar, J. Ravishankar, J. E. Fletcher, and H. R. Pota, "Multi-timescale model predictive control of battery energy storage system using conic relaxation in smart distribution grids," IEEE Transactions on Power Systems (2018).

[21] Y. Zheng, J. Zhao, Y. Song, F. Luo, K. Meng, J. Qiu, and D. J. Hill, "Optimal operation of battery energy storage system considering distribution system uncertainty," IEEE Trans. Sustainable Energy **9**, 1051–1060 (2018).

[22] L. Meng, E. R. Sanseverino, A. Luna, T. Dragicevic, J. C. Vasquez, and J. M. Guerrero, "Microgrid supervisory controllers and energy management systems: A literature review," Renewable and Sustainable Energy Reviews **60**, 1263–1273 (2016).

[23] K. E. Antoniadou-Plytaria, I. N. Kouveliotis-Lysikatos, P. S. Georgilakis, and N. D. Hatziargyriou, "Distributed and decentralized voltage control of smart distribution networks: Models, methods, and future research," IEEE Trans. Smart Grid **8**, 2999–3008 (2017).

[24] Y. Xu, Z. Y. Dong, R. Zhang, and D. J. Hill, "Multi-timescale coordinated voltage/var control of high renewable-penetrated distribution systems," IEEE Transactions on Power Systems **32**, 4398–4408 (2017).

[25] V. Calderaro, V. Galdi, F. Lamberti, and A. Piccolo, "A smart strategy for voltage control ancillary service in distribution networks," IEEE Transactions on Power Systems **30**, 494–502 (2015).

[26] "IEEE standard for interconnection and interoperability of distributed energy resources with associated electric power systems interfaces," IEEE Std 1547-2018 (Revision of IEEE Std 1547-2003) (2018).

[27] R. Tonkoski, L. A. C. Lopes, and T. H. M. El-Fouly, "Coordinated active power curtailment of grid connected PV inverters for overvoltage prevention," IEEE Trans. Sustainable Energy **2**, 139–147 (2011).

[28] S. Ghosh, S. Rahman, and M. Pipattanasomporn, "Distribution voltage regulation through active power curtailment with PV inverters and solar generation forecasts," IEEE Trans. Sustainable Energy **8**, 13–22 (2017).

[29] B. Bletterie, S. Kadam, R. Bolgaryn, and A. Zegers, "Voltage control with PV inverters in low voltage networks–in depth analysis of different concepts and parameterization criteria," IEEE Transactions on Power Systems **32**, 177–185 (2017).

[30] M. J. Reno, J. Deboever, and B. Mather, "Motivation and requirements for quasi-static time series (QSTS) for distribution system analysis," in *2017 IEEE Power Energy Society General Meeting* (Chicago, IL, USA, 2017) pp. 1–5.

[31] L. Ortiz and R. Manghani, "Grid-scale energy storage balance of systems 2015-2020," GTM Research (2016).

[32] R. Deshpande, M. Verbrugge, Y.-T. Cheng, J. Wang, and P. Liu, "Battery cycle life prediction with coupled chemical degradation and fatigue mechanics," Journal of the Electrochemical Society **159**, A1730–A1738 (2012).

[33] P. Fortenbacher, J. L. Mathieu, and G. Andersson, "Modeling and optimal operation of distributed battery storage in low voltage grids," IEEE Transactions on Power Systems **32**, 4340–4350 (2017).

[34] B. Polly, C. Kutscher, D. Macumber, M. Schott, S. Pless, B. Livingood, and O. Van Geet, "From zero energy buildings to zero energy districts," No. NREL/CP-5500-66292 (National Renewable Energy Laboratory (NREL), Golden, CO, USA, 2016).

[35] R. Guglielmetti, D. Macumber, and N. Long, "OpenStudio: An open source integrated analysis platform," in *Proceedings of the 12th Conference of International Building Performance Simulation Association* (Sydney, Australia, 2011) pp. 442–449.

[36] "OpenStudio," `https://www.openstudio.net/`.

[37] C. Christensen, R. Anderson, S. Horowitz, A. Courtney, and J. Spencer, "BEopt™ software for building energy optimization: Features and capabilities," Tech. Rep. NREL/TP-550-

39029 (National Renewable Energy Laboratory, Golden, CO (United States), 2006).
[38] T. Reinhart and C. Cerezo Davila, "Urban building energy modeling a review of a nascent field," Building and Environment **97**, 196 – 202 (2016).
[39] R. C. Dugan, "Reference guide: The open distribution system simulator (OpenDSS)," Tech. Rep. (Electric Power Research Institute, Inc, 2012).
[40] D. W. Gao, E. Muljadi, T. Tian, and M. Miller, "Software comparison for renewable energy deployment in a distribution network," Tech. Rep. TP-5D00-64228 (National Renewable Energy Laboratory, Golden, CO (United States), 2017).
[41] *System Advisor Model Version 2017.9.5 (SAM 2017.9.5)*, National Renewable Energy Laboratory (NREL), Golden, CO, USA (2017), `https://sam.nrel.gov/content/downloads`.
[42] P. Jahangiri and D. C. Aliprantis, "Distributed Volt/VAr control by PV inverters," IEEE Transactions on Power Systems **28**, 3429–3439 (2013).
[43] "Energy standard for buildings except low-rise residential buildings," ANSI/ASHRAE/IES Standard 90.1-2013 (2013).
[44] "U.S. Solar Market Insight Full Report, Q2 2017," GTM Research (2017).
[45] D. Subramanian, J. F. Pekny, and G. V. Reklaitis, "A simulation-optimization framework for addressing combinatorial and stochastic aspects of an R&D pipeline management problem," Computers & Chemical Engineering **24**, 1005 – 1011 (2000).